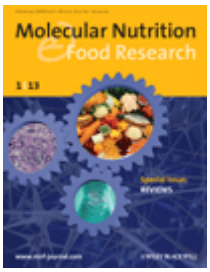

Oxidative stress and dysfunctional intracellular traffic linked to an unhealthy diet results in impaired cargo transport in the Retinal Pigment Epithelium (RPE).

Journal:	*Molecular Nutrition and Food Research*
Manuscript ID	mnfr.201800951.R1
Wiley - Manuscript type:	Research Article
Date Submitted by the Author:	n/a
Complete List of Authors:	Keeling, Eloise; University of Southampton, Clinical and Experimental Sciences, Faculty of Medicine, MP806, Tremona Road, University of Southampton, SO16 6YD, UK. Chatelet, David; University of Southampton, Biomedical Imaging Unit, MP12, Tremona Road, University of Southampton, SO16 6YD, UK Johnston, David; University of Southampton, Biomedical Imaging Unit, MP12, Tremona Road, University of Southampton, SO16 6YD, UK Page, Anton; University of Southampton, Biomedical Imaging Unit, MP12, Tremona Road, University of Southampton, SO16 6YD, UK Tumbarello, David; University of Southampton, Biological Sciences, Faculty of Natural & Environmental Sciences, Life Sciences Building 85, University of Southampton, SO17 1BJ, UK Lotery, Andrew; University of Southampton, Clinical and Experimental Sciences, Faculty of Medicine, MP806, Tremona Road, University of Southampton, SO16 6YD, UK. ; University Hospital Southampton NHS Foundation Trust, Eye Unit Ratnayaka , J. Arjuna; University of Southampton, Clinical and Experimental Sciences, Faculty of Medicine, MP806, Tremona Road, University of Southampton, SO16 6YD, UK.
Keywords:	Cargo trafficking, Phagosome and autophagy-lysosomal pathways, Oxidative stress, Retinal Pigment Epithelium (RPE), Retinopathy

Graphical abstract: text

Oxidative stress and dysfunctional intracellular membrane trafficking are disease processes linked with an unhealthy diet. Here, we demonstrate how these adversely affect the trafficking of photoreceptor outer segment cargos in the Retinal Pigment Epithelium (RPE); a cell layer associated with the neuroretina that is critical to vision. Our discoveries provide new insights into how diet-induced pathogenic mechanisms damage RPE cells which results in irreversible sight loss.

Impaired cargo trafficking in the RPE caused by disease processes linked with an unhealthy diet

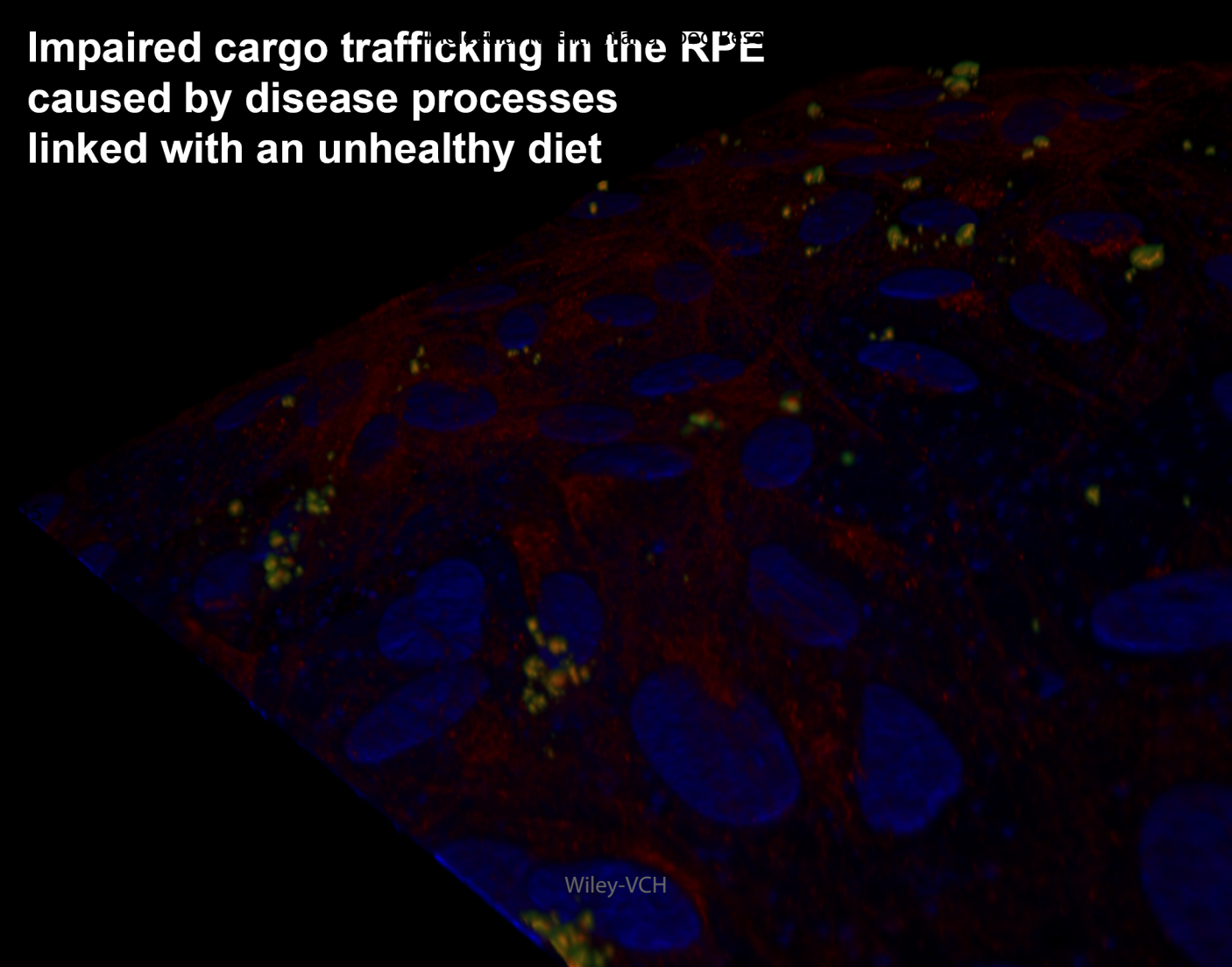

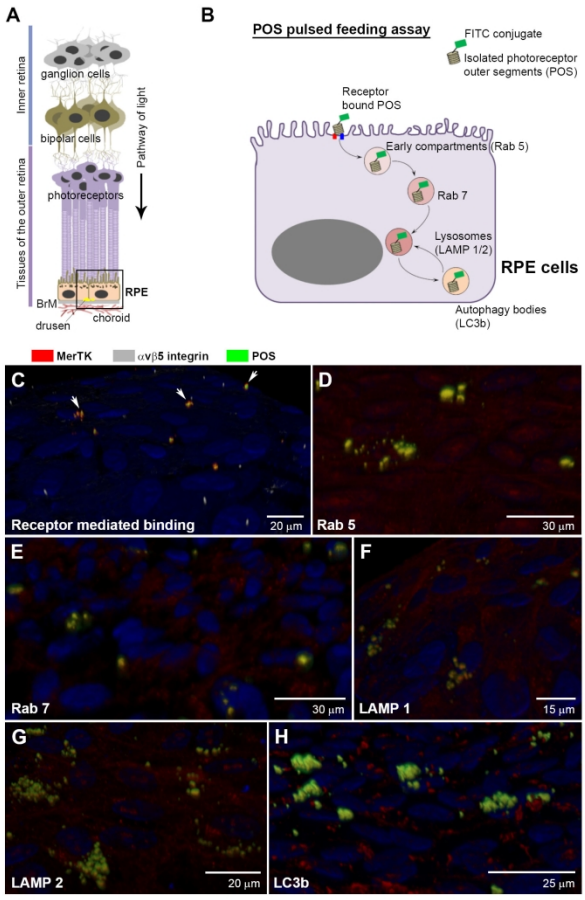

Figure 1

Figure 1

209x297mm (300 x 300 DPI)

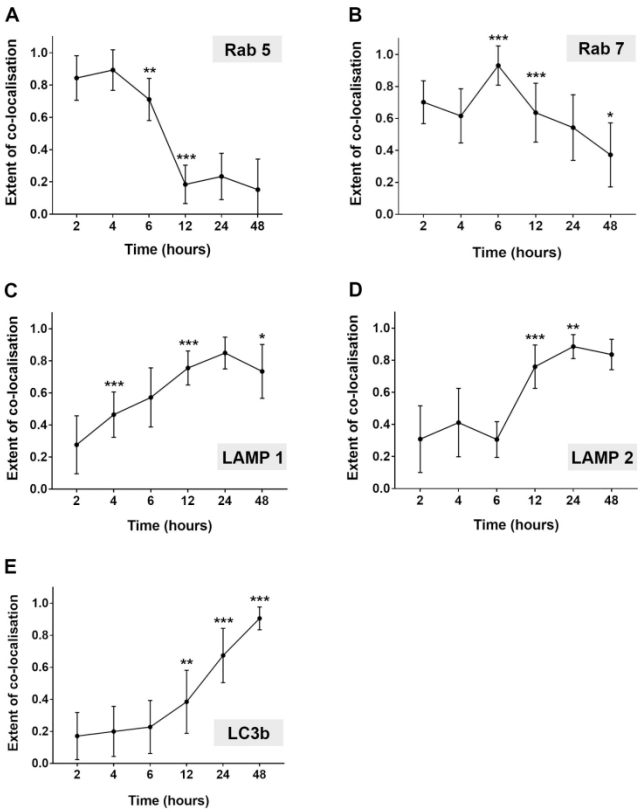

Figure 2

Figure 2

209x297mm (300 x 300 DPI)

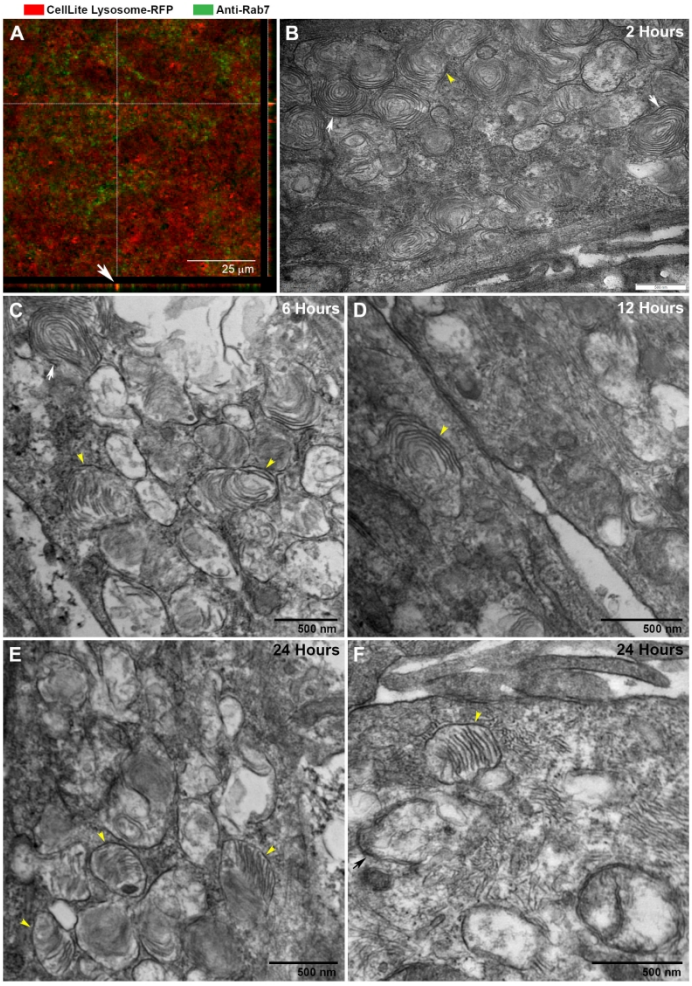

Figure 3

Figure 3

209x297mm (300 x 300 DPI)

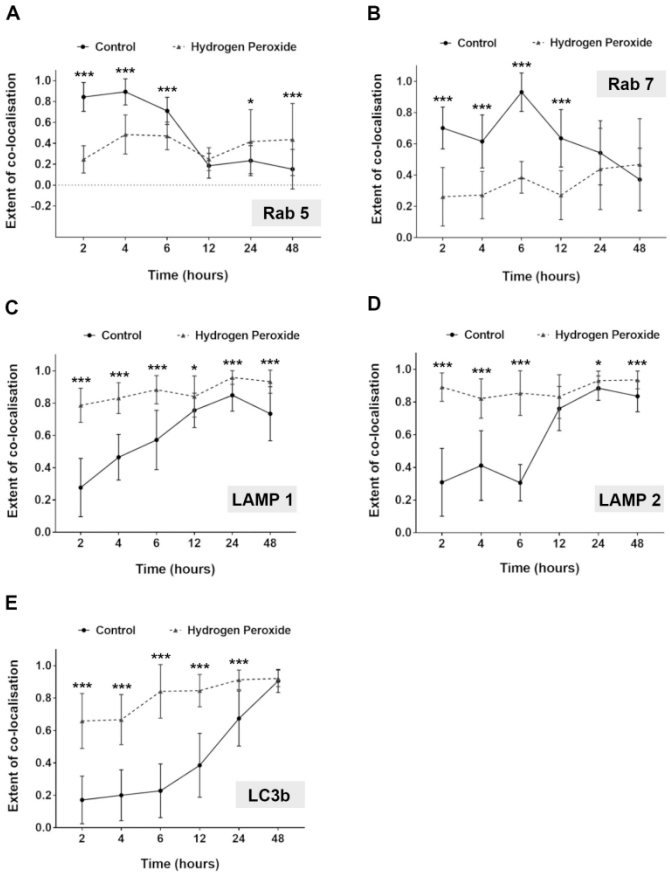

Figure 4

Figure 4

209x297mm (300 x 300 DPI)

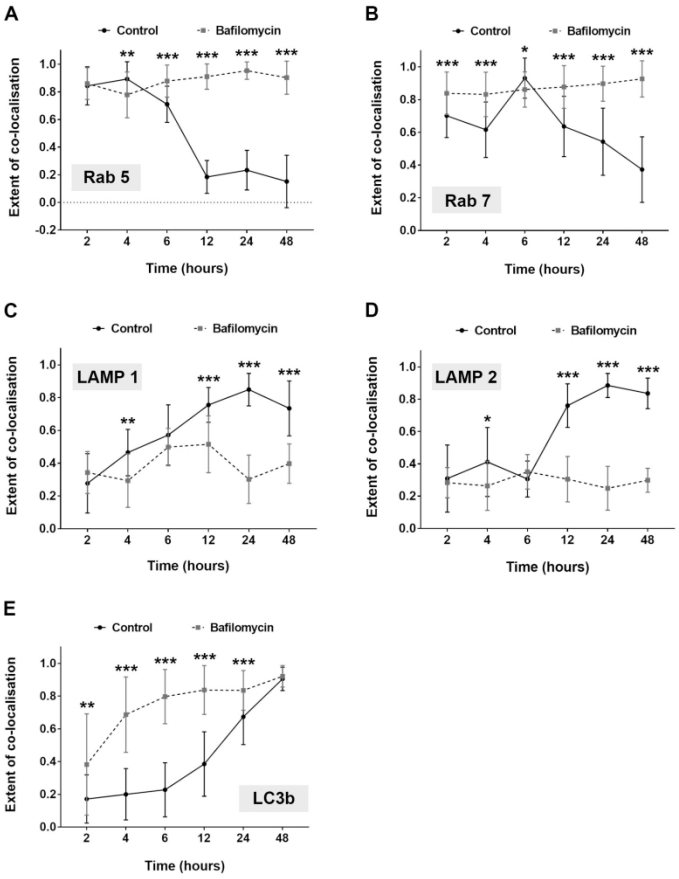

Figure 5

Figure 5

209x297mm (300 x 300 DPI)

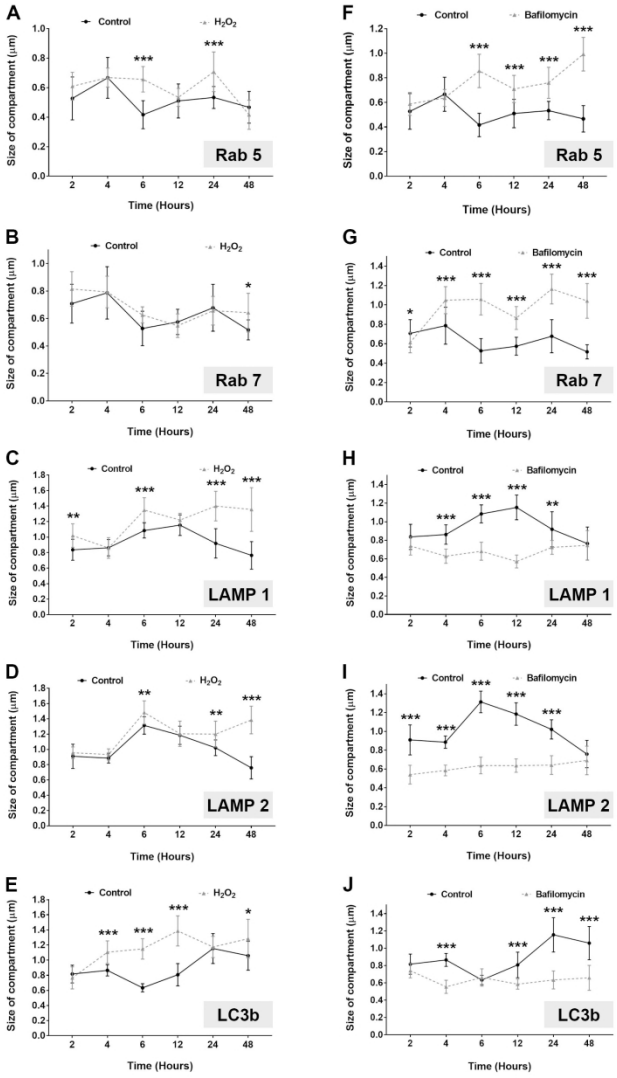

Figure 6

Figure 6

209x297mm (300 x 300 DPI)

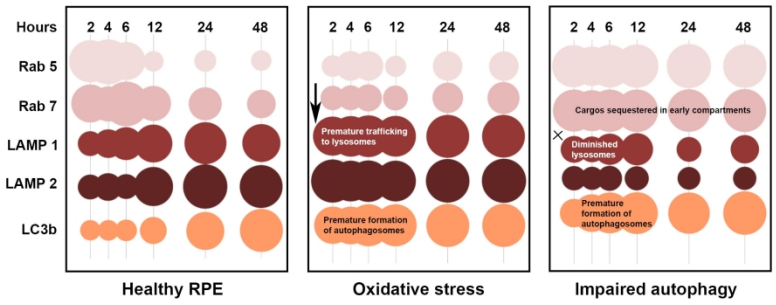

Figure 7

Figure 7

209x297mm (300 x 300 DPI)

Title: **Oxidative stress and dysfunctional intracellular traffic linked to an unhealthy diet results in impaired cargo transport in the Retinal Pigment Epithelium (RPE).**

Eloise Keeling[1], David S. Chatelet[2], David A. Johnston[2], Anton Page[2], David A. Tumbarello[4], Andrew J. Lotery[1,5], J. Arjuna Ratnayaka[1,*]

[1] Clinical and Experimental Sciences, Faculty of Medicine, MP806, Tremona Road, University of Southampton, SO16 6YD, UK.

[2] Biomedical Imaging Unit, MP12, Tremona Road, University of Southampton, SO16 6YD, UK.

[3] Biological Sciences, Faculty of Natural & Environmental Sciences, Life Sciences Building 85, University of Southampton, SO17 1BJ, UK.

[4] Eye Unit, University Hospital Southampton NHS Foundation Trust, Southampton, SO16 6YD, UK.

Keywords: Cargo trafficking, Phagosome and autophagy-lysosomal pathways, Oxidative stress, Retinal Pigment Epithelium (RPE).

Correspondence: * J. Arjuna Ratnayaka (Email: J.Ratnayaka@soton.ac.uk)

Abbreviations: AMD, Age-related Macular Degeneration; **AREDS,** Age-related Eye Disease Study; **BrM,** Bruch's membrane; **GA,** Geographic atrophy; **H_2O_2,** Hydrogen peroxide; **HNE,** 4-hydroxynonenal; **LAP,** LC3-associated phagocytosis; **MDA,** malondialdehyde; **nv,** Neovascular AMD; **A2-E,** N-retinylidine-N-retinylethanolamine; **POS,** Photoreceptor outer segments; **RPE,** Retinal Pigment Epithelium; **TEM,** Transmission Electron Microscopy.

Abstract

Scope: Oxidative stress and dysregulated intracellular trafficking are associated with an unhealthy diet which underlies pathology. Here, we sought to study these effects on photoreceptor outer segment (POS) trafficking in the Retinal Pigment Epithelium (RPE), a major pathway of disease underlying irreversible sight-loss.

Methods and results: POS trafficking was studied in ARPE-19 cells using an algorithm-based quantification of confocal-immunofluorescence data supported by ultrastructural studies. We show that although POS are tightly regulated and trafficked via Rab5, Rab7 vesicles, LAMP1/2 lysosomes and LC3b-autophagosomes, there is also a considerable degree of variation and flexibility in this process. Treatment with H_2O_2 and bafilomycin A^1 revealed that oxidative stress and dysregulated autophagy target intracellular compartments and trafficking in strikingly different ways. These effects appeared limited to POS-containing vesicles, suggesting a cargo-specific effect.

Conclusion: Our findings offer insights into how RPE cells cope with stress, and how mechanisms influencing POS transport/degradation can have different outcomes in the senescent retina. These shed new light on cellular processes underlying retinopathies such as Age-related Macular Degeneration. Our discoveries reveal how diet and nutrition can cause fundamental alterations at a cellular level, thus contributing to a better understanding of the diet-disease axis.

1 Introduction

The intake of a 'Western-style' diet rich in saturated fat, trans-fatty acids, red meat, sodium, fructose and sucrose but low in fibre, plant-derived proteins and mono/polyunsaturated fats are associated with major diseases including diabetes, metabolic disorder and obesity. Typically, these foods are also highly refined and processed. Their consumption is further linked with impaired long-term potentiation and metabolic changes in the brain and degenerative conditions such as Age-related Macular Degeneration (AMD) [1, 2] in which only genetic risk factors were once thought to be drivers of pathology. Dietary intake of such foods is associated with activation of major pathogenic pathways including oxidative stress, the intracellular accumulation and extracellular deposition of lipids and cholesterol as well as dysfunctional clearance mechanisms and chronic inflammation [3, 4]. Here, we focus on studying how high oxidative stress and deregulated intracellular trafficking creates an ideal environment for the development of retinal diseases. Sight loss due to AMD is the most prevalent cause of irreversible blindness in developed societies. The disease manifests as two broadly defined phenotypes referred to as neovascular (nv) AMD which can be treated with regular anti-vascular endothelial growth factor (VEGF) injections, or as geographic atrophy (GA) which has no effective treatment whatsoever [5, 6]. Early AMD, which is largely asymptomatic, is estimated to affect ~150 million individuals globally, whilst the late-stage sight threatening nv/GA forms causes blindness in approximately 10 million patients worldwide [7]. An unhealthy diet contributes to the risk of developing AMD in the same way that a healthier 'Mediterranean' diet or an increased intake of fish and nuts appear to confer protection [2, 8-10]. Therefore, based on initial findings from the Age-related Eye Disease Study (AREDS) some patients are prescribed antioxidants and zinc supplements [11]. Nonetheless, many aspects of this diet-disease axis remain to be elucidated. For instance, how the lack of micronutrients and unhealthy foods trigger disease at the molecular level is still poorly understood [12].

The Retinal Pigment Epithelium (RPE) forms a monolayer of cells underneath the neuroretina whose activities are critical to maintaining lifelong vision (Fig. 1A). Lipid deposition in the Bruch's membrane (BrM) due to the accumulation of esterified cholesterol-rich apolipoprotein B-containing lipoproteins produced by the RPE is a well-characterised feature of early retinopathy [13, 14]. Considerable efforts have therefore focused on studying effects of disease-causing pathways brought about by an unhealthy diet in the RPE. The daily internalisation and proteolytic processing of photoreceptor outer segments (POS) from overlying photoreceptors as part of the visual cycle is a major function of the RPE. The accumulation of partially degraded POS as lipofuscin and its photo-oxidative derivatives in the senescent RPE is a key feature of diseases including AMD and Stargardt disease [15-17]. These lipid/protein aggregates accumulate within RPE lysosomes and related organelles such that approximately 20% of the cell cytosol may be filled with such material by the eighth decade of life [18]. This process occurs in an environment of chronic hypoxia, elevated metabolic activity and cumulative ultraviolet/blue light-induced damage. These changes found in the senescent retina create conditions of high oxidative stress [3, 19, 20]. Risk of disease is exacerbated by the accumulation of lipid/cholesterol aggregates within late endosomes and lysosomes of RPE cells [3, 21]. Autophagy represents a strand of the lysosome-directed degradation pathway and a process by which damaged organelles, misfolded proteins and pathogens are eliminated by the cell. This pathway is also harnessed to recycle cellular constituents in times of starvation. A high fat diet is known to downregulate this pathway by decreasing lysosomal acidity and by reducing fusion between autophagosomes and lysosomes [22, 23]. Here, we sought to separately investigate consequences of high oxidative stress and deregulated intracellular trafficking on POS internalisation and processing which contributes to several forms of retinopathy. We used hydrogen peroxide (H_2O_2) and bafilomycin A^1 to mimic conditions of oxidative stress and impaired lysosomal acidification to study how their effects influence the ability of RPE to traffic POS cargos.

Our discoveries not only provide new information on the dynamic manner in which cargos are processed in the phagosome and autophagy-lysosomal pathways of RPE cells, but also a nuanced breakdown of POS trafficking at each time point. The tightly regulated passage of cargos via Rab5, Rab7 compartments, LAMP1/2 lysosomes and LC3b labelled autophagosomes is offset by a certain level of variability, indicating some flexibility in this process. This was nonetheless severely disrupted following exposure to H_2O_2 and bafilomycin A[1] which induces elevated oxidative stress and deregulated intracellular membrane trafficking. These insults were also correlated with significant changes to the size of POS-containing compartments. Interestingly, the size of Rab5, Rab7, LAMP1/2 vesicles and autophagosomes without POS in treated cultures remained unaffected. Our findings quantifiably demonstrate the subtle cellular mechanisms that are affected in the diet-disease axis, and how heathy RPE could switch to the diseased phenotype.

2 Material and methods

2.1 Cell culture

The non-transformed human cell line ARPE-19 [24] was obtained from the American Tissue Culture Collection (ATCC, USA) and maintained in a 37°C humidified incubator with 5% CO_2 and 95% air. Cells were routinely cultured in Dulbecco's modified Eagle's medium (DMEM) with 4.5g/l L-D glucose, L-glutamine and pyruvate (Life Technologies, UK), supplemented with 1% heat-inactivated foetal calf serum (Sigma Aldrich, UK) and 1% penicillin-streptomycin stock solution (10,000 units/ml penicillin, 10mg/ml streptomycin in 0.85% saline; Sigma Aldrich, UK) [25]. Cells cultured in a T25 flask were maintained in a 5ml volume of medium, with a complete media change performed every 3-4 days. Post confluent ARPE-19 cultures between passages 10-25 were maintained for up to 4 months prior to seeding on 0.4µm pore PET polyester transwell inserts (Sigma Aldrich, UK) pre-coated with 50µg/ml fibronectin (Sigma-Aldrich, UK). ARPE-19 cells were seeded at a density of $1.25x10^4$ cells/well on 12mm diameter inserts. Cells were maintained in 0.5ml and 2ml

media volumes in apical and basal chambers respectively. A complete medium change in the apical compartment and a 20% (v) change in the basal compartment was performed every 3-4 days. Cells were cultured for a minimum of 4 months prior to use in experiments [26].

2.2 Photoreceptor outer segment (POS) pulse assay

Retinas were isolated from porcine eyes and pooled in KCl buffer (0.3M KCl, 10mM HEPES, 0.5mM $CaCl_2$, 2mM $MgCl_2$) in 48% sucrose solutions. Collected retinas were homogenised by gentle shaking for 2min. The solution was then centrifuged at 5000xg for 5 minutes before the supernatant was passed through a sterile gauze into fresh centrifuge tubes and diluted with KCl buffer without sucrose. This preparation was subsequently centrifuged at 4000xg for 7 minutes after which the pellet was washed 3 times in PBS through centrifugation at 4000xg for a further 7 minutes. POS were resuspended in 20mM phosphate buffer (pH 7.2) with 10% sucrose and 5uM taurine. The FITC conjugate (ThermoFisher, UK) was added and the solution was left on a rotating plate for 1 hour in the dark to allow for covalent attachment of the fluorescent tag. The POS-FITC solution was then centrifuged at 3000xg for 4 minutes at 20^{o}C, suspended in DMEM with 2.5% sucrose, aliquoted and stored at -80^{o}C. Isolated POS were quantified using a BCA assay (Pierce, ThermoFisher, UK) in which proteins were measured against standards between 20-2000µg/ml via absorption at 562nm (Infinite F200 Pro, Tecan, Switzerland). Cultures were pre-treated with either 10nM Bafilomycin A[1] (Tocris, UK) for 48 hours [27] or 100µM hydrogen peroxide (H_2O_2; Sigma Aldrich, UK) for 24 hours [28, 29] before feeding with POS. Untreated sister cultures acted as controls. RPE monolayers were chilled to17^{o}C for 30 minutes and pulsed with POS as describe before [30]. We used 4µg/cm^2 of POS-FITC [31], after which cultures were left at 17^{o}C for a further 30 minutes to maximise binding whilst minimising any cargo internalisation. The medium was aspirated to remove unbound POS, replaced with fresh pre-warmed medium and cultures returned to a humidified incubator at 37^{o}C with 5% CO_2.

2.3 Confocal immunofluorescence microscopy and image analysis

Cultures were fixed in 4% formaldehyde (in 0.1M phosphate-buffered saline [PBS]) for 30 minutes at 4°C, permeabilised in 0.1% Triton-X 100 for 30 minutes and blocked in PBS containing 1% BSA and 0.1% Tween for a further 30 minutes. Cells were then incubated with primary antibody diluted in the same solution at 4°C overnight. Cultures were probed with the following antibodies: rabbit-anti Rab5 (AB_470264; 1:200), rabbit anti-Rab7 (AB_2629474; 1:200), rabbit anti-LAMP1 (AB_775978; 1:1000), rabbit anti-LAMP2 (AB_755981; 1:1000), rabbit anti-LC3b (AB_881433; 1:200), rabbit anti-MerTK (AB_10863559; 1:100) and mouse anti- αVβ5 integrin (AB_448231; 1:100). Following removal of unbound antibodies by washing, cells were incubated for 1 hour at room temperature with Alexa Fluor-conjugated secondary antibodies (AB_2534116, AB_2534085) in a dilution of 1:100 in PBS-Tween with BSA and cytopainter phalloidin-iFluor 647 (Ab176759, Abcam, UK; 1:1000). In all instances 1µg/mL of 4',6'-diamino-2-phenylindole (DAPI; D9542, Sigma Aldrich, UK) was used to visualise cell nuclei. Samples were mounted between two glass coverslips using Mowiol, and images acquired using a Leica SP8 (Leica Microsystems, UK) confocal laser scanning microscope. Quantification of POS-FITC in various intracellular compartments was carried out using Volocity software (Perkin Elmer, UK) which uses an automated, unbiased statistical algorithm [32]. Images were randomly selected from a database collected across three independent experiments (n≥20 cells/compartment/time point for untreated controls and n≥15 cells/compartment/time point for treated groups). Co-localisation values were plotted for each compartment as a function of time. For labelling lysosomes, 2µl CellLite™ Lysosomes-RFP (Life Technologies, UK) was applied per 10,000 cells and incubated for a period of 24 hours. The size of intracellular compartments was measured by ImageJ software (NIH, USA) using single plane images from the middle of confocal z-stacks at 200x magnification; n=15, with separate measurements for each compartment/time point/treatment. Images were selected at random from a database collected across three independent experiments and size measurements

carried out using only the red channel (vesicle marker). POS containing vesicles were pre-identified and the green channel (POS) switched off to remove the fluorescence flare interfering with measurements.

2.4 Transmission electron microscopy (TEM)

After RPE monolayers were pulsed with POS, cultures were fixed with primary fixative comprising 3% glutaraldehyde, 4% formaldehyde in 0.1M PIPES buffer (pH 7.2) for a minimum of 1 hour. Specimens were then rinsed in 0.1M PIPES buffer, post-fixed in 1% buffered osmium tetroxide for 1 hour, rinsed in buffer and block-stained in 2% aqueous uranyl acetate (20 minutes). Samples were then dehydrated in an ethanol gradient (30%, 50%, 70%, 95%) for 10 minutes each and twice in absolute ethanol for 20 minutes. The link reagent acetonitrile was then applied for 10 minutes after which samples were incubated overnight in a 1:1 ratio of acetonitrile to Spurr resin. The following day cells were incubated in fresh Spurr resin for 6hr before being embedded and polymerised in Spurr resin (Agar Scientific, Stanstead, UK) at 60^{o}C for 24 hours. Silver/gold ultrathin sections were cut on a Reichert Ultracut E ultramicrotome (Leica Microsystems, UK), collected on 200 mesh copper grids and stained with Reynolds lead stain. Sections were viewed using a Hitachi HT7700 (Hitachi High Technology, Japan) Transmission Electron Microscope. Analysis was carried out in blinded micrographs where n≤20 images were collected for each time point. The extent of cargo degradation in electron micrographs were anonymised and evaluated based on; (1) no evidence of POS degradation within vesicles, (2) where POS cargos showed signs of breakdown associated with presence of electron-dense material, or (3) where degraded POS with electron-dense material were localised to lysosomes and/or autophagy bodies [33]. POS positive vesicles in micrographs were also quantified based on distance from the apical RPE surface (measured from the apical cell membrane to the nearest edge of the vesicle).

2.5 Statistical analysis

Statistical comparisons were performed using GraphPad prism Software (GraphPad, CA, USA). The statistical differences were determined using an unpaired Student t-test or a one-way ANOVA. Data is expressed as a mean value ± standard deviation (SD) where significance is denoted by a * for $p \leq 0.05$, ** for $p \leq 0.01$ or *** for differences of at least $p \leq 0.001$.

3 Results

3.1 The trafficking of POS cargos in heathy RPE cells.

In order to study how POS molecules were trafficked in the RPE we exploited a well-characterised cell model which recapitulates key structural and physiological features of their native counterpart [26, 34]. Use of an *in-vitro* system allowed a high degree of experimental manipulation as well as unimpeded access to high-resolution microscopes and live cell imaging capabilities. We used a modified feeding assay to maximise POS binding whilst synchronising internalisation to monitor the trafficking process [30]. Fluorescently tagged POS molecules were used to track initial binding followed by trafficking through phagosomes/endosomes and the lysosomal-autophagy pathway (Fig. 1B and Supplementary Fig. S1). Following a washing step in which excess POS was removed, we found no evidence of any unbound POS on cells. Co-labelling with antibodies showed that POS binding was mediated via MER receptor tyrosine kinase (MerTK) and $\alpha v\beta 5$ integrin receptors. Furthermore, all bound POS were associated with receptor complexes, although those that had not bound to any cargo (typically isolated receptors) were also visible (Fig. 1C). Four hours after commencing the feeding assay, POS were observed localised to Rab5 labelled early compartments (Fig. 1D). Six hours after the assay had begun, cargos were found in Rab7 vesicles corresponding to late phagosomes/endosomes (Fig. 1E). Although representative images are shown for each compartment, during initial stages of trafficking cargos are likely to move through a mixture of Rab5 and Rab7 vesicles at any given time point. However, 24 hours after the feeding assay, most cargos were localised to LAMP1

early lysosomes (Fig. 1F) or LAMP2 mature lysosomes (Fig. 1G). POS in lysosomes had a predominantly perinuclear arrangement, consistent with findings that cargos intended for degradation are trafficked to lytic compartments deeper in the cell and in proximity to the nucleus [35]. By 48 hours, most POS molecules had co-localised to LC3b labelled compartments, which also had a largely perinuclear distribution (Fig. 1H). In order to quantify trafficking of POS cargos through distinct intracellular vesicles we used an automated statistical method described by Costes *et al* [32]. This algorithm provides an unbiased assessment of the number of POS molecules co-localising with each intracellular marker. The extent of POS in each compartment is shown as a fraction where a value of 1.0 represents 100% co-localisation. During the first 2-4 hours after POS feeding, a large proportion of cargos were observed co-localised with Rab5 early compartments. The extent of co-localisation dropped significantly thereafter and from 12 hours onwards only a small proportion remained in Rab5 vesicles (Fig. 2A). Assessment of cargo trafficking using the Rab7 marker indicated that the highest extent of co-localisation was at 6 hours. POS levels within Rab7 compartments dropped significantly thereafter. Surprisingly, a substantial proportion (~50% co-localisation) of cargos remained within Rab7 vesicles as late as 24 hours after POS pulse (Fig. 2B and Supplementary Table 1). Quantification of POS trafficked to LAMP1 early lysosomes showed a gradual increase of cargos with the highest extent of co-localisation 24 hours after the pulse (Fig. 2C). In contrast, only low levels of POS co-localised with LAMP2 compartments during initial stages (up to 6 hours) after which ~90% of cargos had trafficked to mature lysosomes by 24 hours (Fig 2D and Supplementary Table 1). Levels of POS in LC3b labelled membranes were also initially observed to be at low levels but increased significantly from 12 hours onwards to reach a maximal extent of co-localisation of ~90% by 48 hours (Fig 2E and Supplementary Table 1). Our quantification thus provided valuable new information on how POS cargos are sequentially trafficked through each intracellular compartment in heathy RPE cells.

3.2 Labelling of intracellular vesicles using probes and assessment of POS trafficking by ultrastructural microscopy.

Although Rab7 labelling can distinguish between late phagosomes/endosomes vs. lysosomes, there is evidence to suggest that some lysosomes are also positive for Rab7 [35-37]. In order to assess whether this occurs in the RPE, living cells were transfected with a genetic lysosomal marker after which they were probed with an antibody specific for Rab7. Although a majority of late vesicles were labelled for either Rab7 or lysosomes, on occasion we observed the co-localisation of these two respective markers to a single compartment (Fig. 3A). Next, we assessed the passage of POS through different intracellular compartments by electron microscopy. The trafficking of cargos at each time point was captured in a series of micrographs by a blinded assessor which revealed that most POS were localised to early compartments at 2 hours. POS remained largely intact within these vesicles with little evidence of significant degradation (Fig. 3B). Between 6 and 12 hours however, most cargos showed some evidence of breakdown (Fig. 3C,D). By 24 hours, cargos exclusively appeared in late compartments/lysosomes containing a mixture of POS and associated electron dense material showing further signs of degradation (Fig. 3E,F). The appearance of double membrane structures at the 24 hour time point indicated formation of autophagosomes associated with terminal stages of the proteolytic pathway (Fig. 3F). Quantification of POS degradation in electron micrographs showed increasing levels of cargo breakdown correlated with time (Supplementary Fig. S2). Moreover, a higher incidence of POS breakdown was correlated with increasing distances from the apical surface along the apical-basal axis of RPE cells (Supplementary Fig. S3). POS positive compartments with no signs of cargo degradation were predominantly found in proximity to the apical RPE surface, whilst vesicles with POS in advanced stages of breakdown were localised to the perinuclear region and in proximity to the basolateral RPE membrane (Fig. S4).

3.3 Oxidative stress causes the rapid and premature trafficking of POS to late compartments.

We studied potential effects of high oxidative stress on POS trafficking by exposing cultured RPE to 100μM H_2O_2. We observed a marked decrease of cargos in Rab5 early compartments in cells treated with H_2O_2 compared to untreated sister cultures (on average only 38% of cargos were trafficked in Rab5 vesicles throughout the experiment under conditions of oxidative stress compared to 50% in heathy cells). However, the extent of co-localisation in Rab5 vesicles increased at 24 and 48 hours in H_2O_2 treated cells compared to controls (Fig. 4A). A similar pattern of low level POS co-localisation was observed in Rab7 compartments compared to untreated cultures (on average only 35% of cargos were trafficked in Rab7 vesicles throughout the experiment under conditions of oxidative stress vs 63% in heathy controls) (Fig. 4B and Supplementary Table 1). By contrast, approximately 80% of POS had co-localised to LAMP1 compartments after just 2 hours in RPE exposed to high levels of oxidative stress (compared to only 28% in untreated cultures at the same time point). Moreover, the extent of co-localisation in early lysosomes remained consistently high thereafter with a maximal value of 96% recorded 24 hours after POS pulse (Fig. 4C). We also observed high levels of POS co-localisation in LAMP2 positive compartments (89% compared to only 31% in controls at the 2 hour time point). Elevated levels of POS continued to localise to these mature lysosomes at subsequent time points to reach a maximal value of 94% by 48 hours after POS pulse (Fig. 4D and Supplementary Table 1). Under conditions of elevated oxidative stress, cargos also localised prematurely to LC3b labelled compartments compared to untreated cultures (66% compared to only 17% in controls at the 2 hour time point). High levels of cargos remained associated with LC3b labelled membranes thereafter and increased significantly at subsequent time points to reach a maximal value of ~90% (at which time point cargos in LC3b compartments in control cultures had also reached similar levels). (Fig. 4E and Supplementary Table 1). Our findings thus revealed the contrasting fate of POS trafficked in cells subject to oxidative stress compared to untreated/healthy RPE.

3.4 Dysregulated intracellular trafficking leads to POS being sequestered in early compartments.

Impairment of the autophagy pathway was induced by exposing cells to bafilomycin A[1], which disrupts acidification of intracellular compartments thus hindering fusion events along the phagosome/endosomal and autophagy pathways. Cultured RPE were treated with 10nM bafilomycin after which the extent of POS trafficking in each compartment was quantified as before. Cargos were initially observed to localise with Rab5 labelled vesicles, equivalent to levels recorded in untreated cultures. However, in bafilomycin treated cells, cargos continued to be associated with Rab5 vesicles at subsequent time points long after they had been trafficked to downstream compartments in untreated/heathy RPE. We recorded a maximal extent (95%) of POS co-localised with these early compartments at 24 hours in bafilomycin treated cells compared to only 23% in control RPE at the same time point (Fig. 5A and Supplementary Table 1). A similar pattern was observed in Rab7 labelled vesicles, where on average 87% of cargos had been trafficked throughout the experiment in bafilomycin treated cells compared to only 63% in heathy RPE. Cargos continued to be sequestered in Rab7 compartments at late time points with the highest extent of co-localisation recorded at 48 hours (93%) compared to only 37% in control cells at the same time point (Fig. 5B and Supplementary Table 1). Assessment of LAMP1 labelled compartments revealed diminished levels of POS compared to heathy RPE. When vesicle maturation was disrupted, on average only 39% of cargos were trafficked to early lysosomes throughout the experiment compared to 61% in heathy RPE. This discrepancy was particularly evident 12 hours after the POS pulse when most cargos had been trafficked to lysosomes under normal circumstances (Fig. 5C). In cultures treated with bafilomycin, a similar pattern was observed in LAMP2 labelled compartments which contained only low levels of POS compared to untreated cells. This was evident 12 hours after the POS pulse had commenced, when heathy RPE had trafficked a large proportion of cargos to mature lysosomes. Consequently, on average only 29% of cargos co-localised to LAMP1 vesicles throughout the experiment compared to 58% in untreated/control cells (Fig. 5D and

Supplementary Table 1). Quantification of POS in LC3b labelled compartments however revealed higher levels of co-localisation to autophagosomes from early time points in cells treated with bafilomycin compared to heathy RPE. Association with LC3b labelled membranes remained significantly high at subsequent time points compared to untreated cells. However, 48 hours after the POS pulse had commenced, the extent of cargos in LC3b compartments were similar in both treated and control cultures (Fig. 5E). Our findings thus reveal biphasic effects of dysregulated vesicle maturation with some POS being sequestered in early compartments whist another proportion of cargos appear to be prematurely directed to LC3b labelled membranes.

3.5 Oxidative stress and dysregulated membrane trafficking affects the size of intracellular compartments in the POS trafficking pathway.

As abnormalities in endosomes and lysosomes are reported to be indicators of incipient pathology, we studied whether elevated oxidative stress and impaired intracellular trafficking could alter the size of compartments in the POS trafficking pathway. Exposure to 100μM H_2O_2 resulted in significantly larger Rab5 labelled vesicles at 6 and 24 hours compared to untreated cells (Fig. 6A and Supplementary Table 2). In earlier studies, elevated levels of POS co-localised with Rab5 at the 24 and 48 hour time points (Fig. 3A). We noticed that larger Rab5 vesicles correlated with this increase at 24 hours but there were no appreciable differences in vesicle size by 48 hours. Analysis of Rab7 vesicles showed that exposure to H_2O_2 had produced no appreciable effects on the size of these compartments bar at 48 hours when significantly larger Rab7 vesicles were recorded (Fig. 6B). However, measurement of LAMP1 positive lysosomes containing POS revealed a significant increase in size following exposure to H_2O_2. This was evident from the first time point at 2 hours when lysosomes were 1.02μm ±0.15 compared to 0.84μm ±0.14 in heathy RPE. At time points at which significant differences were recorded, the average size of these early lysosomes measured 1.28μm ±0.21 compared to 0.92μm ±0.16 in untreated cells (Fig. 6C,

Supplementary Fig. S5 and Table 2). Swollen LAMP1 vesicles also correlated with abnormally high POS from an early time point (Fig. 3C). We observed a similar pattern of enlarged LAMP2 vesicles in cells exposed to H_2O_2. However, this was evident only at later time points. Where significant differences were recorded, the average size of mature lysosomes measured 1.36μm ±0.17 compared 1.03μm ±0.12 in untreated cells with the most difference at 48 hours (1.39μm ±0.18 compared to 0.76μm ±0.15 in heathy RPE) (Fig. 6D and Supplementary Table 2). This may reflect the rapid/premature POS trafficking to LAMP2 compartments under conditions of oxidative stress (Fig. 3D). Quantification of LC3b labelled autophagosomes revealed significant increases in their size between 4-12 and at 48 hours under oxidative stress with average sizes of 1.23μm ±0.19 vs. 0.84μm ±0.12 in heathy RPE at these time points. The most significant size difference in autophagosomes between H_2O_2 vs. untreated cultures was recorded at 6 hours (1.15μm ±0.14 vs 0.63μm ±0.05, respectively) when most cargos had not yet reached these compartments under normal circumstances (Fig. 6E and Supplementary Table 2). The increased size of LC3b labelled vesicles broadly correlated with premature POS localisation to these compartments (Fig. 3E). Where significant differences in the size of compartments were recorded between H_2O_2 exposed and control cultures, we also measured the size of fluorescent vesicles without any POS cargo (Supplementary Table 3). We were surprised to find that the size of respective compartments in treated cultures remained unaffected and similar to the size of their counterparts in untreated/heathy RPE.

Next, we studied whether exposure to bafilomycin affected the size of intracellular compartments in the POS trafficking pathway. Measurement of POS containing Rab5 vesicles, at time points where significant differences in co-localisation was recorded, showed a marked increase in size after 6 hours with an average value of 0.83μm ±0.13 compared to 0.48μm ±0.1 in heathy RPE (Fig. 6F and Supplementary Table 2). We noticed that enlarged Rab5 vesicles correlated with time points at which elevated POS was also trafficked to these

early compartments (Fig. 4A). Analysis of Rab7 compartments showed initially smaller vesicles (at the 2 hour time point) becoming larger from 4 hours onwards compared to controls. At time points in which significant increases were recorded in co-localisation, the average size of enlarged Rab7 vesicles measured 1.04μm ±0.15 compared to 0.62μm ±0.13 in heathy RPE (Fig. 6F and Supplementary Fig. S5). Enlarged Rab7 vesicles broadly correlated with elevated POS trafficking to these compartments particularly at later time points (Fig. 4B). In contrast to enlarged Rab5 and Rab7 compartments, we observed a marked reduction in the size of LAMP1 vesicles with POS. Although there were no differences at the initial 2 hour time point, the size of early lysosomes were substantially smaller between 4-24 hours. At time points where significant differences were recorded in co-localisation, their average size measured only 0.65μm ±0.08 compared to 1.05μm ±0.15 in heathy RPE. The abnormal size of small lysosomes had returned to normal levels by 48 hours (Fig. 6H and Supplementary Table 2). Fluctuations in the size of LAMP1 compartments corresponded with time points at which diminished POS levels co-localised to these organelles (Fig. 4C). A broadly similar pattern was observed in LAMP2 compartments which were significantly smaller between 2-24 hours compared to those in control RPE cells. Measurement of mature lysosomes at these time points showed an average size of 0.61μm ±0.08 compared to 1.06μm ±0.11 in RPE where autophagy was normal. The size of LAMP2 compartments had returned to normal levels by 48 hours (Fig. 6I and Supplementary Table 2). Variations in the size of mature lysosomes broadly corresponded with diminished POS trafficking to these compartments, particularly at late time points (Fig. 4D). Measurement of LC3b membranes with POS showed smaller sized autophagosome at 4, 12, 24 and 48 hours compared to controls. Their average size at these time points corresponded to 0.61μm ±0.09 compared to 0.97μm ±0.15 in heathy RPE cells (Fig. 6J and Supplementary Table 2). In a marked contrast to the broad correlation between vesicle size and the extent of co-localisation in Rab5, Rab7 and LAMP1/2 lysosomes, we found that smaller LC3b compartments in fact generally appeared to have a significantly higher incidence of POS

labelling (Fig. 4E). Where significant size differences were recorded between bafilomycin treated and untreated cultures, we also measured the size of compartments without any POS cargos, which revealed normal sized vesicles in treated cells (Supplementary Table 3). Our studies thus reveal new information on how distinct compartments in the POS trafficking pathway respond to different insults in RPE cells.

4 Discussion

Understanding the molecular mechanisms through which an unhealthy diet results in pathogenic alterations at the cellular level has become an area of increasing importance, especially in light of age-related diseases such as AMD. Here, we explored how this diet-disease axis could cause retinal damage by studying pathogenic processes associated with a 'Western-style' diet in the RPE. Epidemiological studies demonstrate a link between a diet rich in red/processed meat, high-fat dietary products, fried foods, refined grains and eggs with developing AMD [2, 10, 12]. These findings are supported by new evidence highlighting the importance of cholesterol metabolism in the retina [4]. Elegant studies have used animal models to garner considerable insights into these mechanisms. For example, wildtype rabbits and mice given a high fat-cholesterol enriched diet develop astrogliosis, drusen-like debris, RPE-BrM abnormalities, elevated Amyloid beta (Aβ), oxysterols and retinal cholesterol deposits as well as impaired retinal function [38-41]. Human ApoE4 knock-in mice that were aged and switched to a 'Western-style' diet develop ApoE and Aβ containing sub-RPE deposits, a thickened BrM, RPE atrophy opposed to photoreceptor degeneration and choroidal neovascularisation as well as functional retinal defects [42]. By exploiting *in-vitro* models these studies can be extended to understand how an unhealthy diet affects specific tissues at cellular level. Studies in Abca4$^{-/-}$ mice showed that elevated cholesterol impairs microtubule-mediated lysosomal trafficking and CD59 transport to the RPE surface, thereby compromising the ability to defend against complement attack [43]. Moreover, the lipofuscin derivative N-retinylidine-N-retinylethanolamine (A2-E) impairs efflux of cholesterol

from late endosomes/lysosomes leading to the accumulation of cholesterol esters in RPE, providing further evidence for dysfunctional cholesterol metabolism [21]. Cultured RPE are capable of producing subcellular deposits rich in apolipoprotein, complement proteins and other drusen constituents [44], demonstrating the effectiveness of cell models for studies of this kind. Oxidised lipoproteins accumulate in the aging BrM prior to the development of pathogenic sub-RPE deposits and drusen [14]. Oxidised phospholipids, a component of oxidised lipoproteins, are generated by lipid peroxidation of highly polyunsaturated fatty acids in photoreceptors [45]. Such phospholipids subsequently accumulate in the macula and increase with age and in eyes with AMD [46]. *In-vitro* studies show that oxidised phospholipids block the activity of phosphatidylinositol 3-kinase to cause a delay in the acquisition of lysosomal markers by newly formed RPE phagosomes [47]. Lipid peroxidation of POS membranes also results in modified products 4-hydroxynonenal (HNE) and malondialdehyde (MDA) in lipofuscin isolated from donor RPE [48]. HNE and MDA modification significantly impairs POS breakdown in lysosomes resulting in the intracellular accumulation of undigested cargo [49, 50]. Modified POS also acts as a proteolytic antagonist by inhibiting activities of lysosomal enzymes to bring about a reduction of lysosomal proteolytic capacity in the RPE [51]. There is also evidence to show that a 'Western' diet significantly increases free radical-mediated oxidative damage in the retina [3, 29]. This may contribute substantially to chronic oxidative stress, as the retina is an ideal environment for generating hydrogen peroxide, singlet oxygen and superoxide anion species amongst others. Polyunsaturated fatty acids in POS for instance are particularly susceptible to free radical damage [19].

The daily internalisation and proteolytic processing of POS by RPE cells in the phagosome and autophagy-lysosomal pathways and its dysfunction is linked with retinopathies including AMD, Stargardt disease and choroideremia [15-17, 43, 52-54]. Photoreceptors shed ~10% of their distal tips on a daily basis which are engulfed by the underlying RPE [55]. Studies in non-human primates reveal that a single RPE cell in the parafovea is exposed to 2000 discs

daily, whilst exposure in the perifovea and periphery approximate to 3500 disks and 4000 disks respectively, with each RPE processing up to a billion photoreceptor disks over a 70 year period [56]. This makes the RPE one of the most proteolytically stressed tissues in the body. POS cargos have been shown to bind RPE within 1-2 hours, be engulfed between 4-6 hours and digested within a period of 16-20 hours following initial POS challenge [21, 57]. As POS binding to $\alpha v\beta 5$ integrin stimulates focal adhesion kinase to activate MerTK [58], we first confirmed that POS internalisation in our assay was mediated via these receptors. We used POS feeding coupled to a pulse assay to maximise the extent of cargo binding whilst minimising its premature internalisation, thus synchronising POS trafficking in order to track temporal changes [30]. We labelled the major early, intermediate and late compartments in the trafficking pathway to obtain a dynamic and nuanced picture of POS degradation in heathy RPE cells. For the first time we can visualise the sequential trafficking of POS cargos by 3D-rendered confocal immunofluorescence microscopy. We utilized an algorithm widely employed in studies of this kind to automatically and objectively quantify the extent of POS co-localisation in each compartment [32], which revealed temporal dynamics of this process in an unprecedented manner. Early trafficking to Rab5 vesicles reached a peak at 4 hours, after which cargos peaked in Rab7 compartments by 6 hours. Surprisingly, POS positive Rab7 vesicles were evident even at late time points (24-48 hours) when cargos are expected to have been trafficked through mature phagosomes and endosomes. However, co-labelling studies using a Rab7 specific antibody as well as a lysosomal probe indicated that some lysosomes were also positive for Rab7, which may account for this observation. The internalisation of POS in early compartments was also assessed by electron microscopy, which initially showed little or no evidence of degradation. However, there were some signs of POS breakdown by 6-12 hours by which time immunofluorescence studies revealed most cargos to be in Rab7 late phagosomes/endosomes. POS started to appear incrementally in early lysosomes, and significantly at later time points in mature lysosomes. POS reached a peak in both LAMP1/2 lysosomes by 24 hours. This was consistent with ultrastructural data which showed the appearance of degraded POS associated with electron dense material

indicating further processing in the proteolytic pathway. Quantification of cargo processing in electron micrographs were based on the extent of POS breakdown, as well as the reported morphology of lysosomes [33]. Moreover, POS proteolysis appeared to occur along the apical-basal axis of RPE cells, with the highest level of degradation within compartments in proximity to the basolateral membrane. Cargos finally co-localised with LC3b labelled compartments, initially at low levels during early time points (2-6 hours), but increased significantly after 12 hours to reach of peak by 48 hours. Electron micrographs taken at 24 hours captured double-membrane autophagosomes that typically associate with LC3-II in conventional autophagy [59], further demonstrating the transfer of POS to terminal stages of the proteolytic pathway. Our detailed breakdown of POS trafficking in healthy RPE was in-line with broad timeframes in which these cargos are reportedly engulfed and degraded [21, 57, 60]. Our studies also show the dynamic nature of POS trafficking and insights into how some intracellular compartments can have multiple identities or markers, perhaps indicating transition states or multiple functions. This would be consistent with recent discoveries that reveal new roles for lysosomes and the different ways in which intracellular compartments communicate with each other [35-37, 61, 62]. Importantly, our findings revealed that although a majority of POS cargos are tightly shuttled via Rab5, Rab7 and LAMP1, 2 and LC3b compartments in heathy RPE, there is also a considerable degree of flexibility and variation in this process. Such insights contribute to the current understanding of how cargos are trafficked and processed in the RPE. Although we and others have utilised well-characterised approaches to ensure a tight pulse [26, 30, 34, 35, 60], the possibility of some premature POS internalisation due to leakage cannot be fully excluded. However, it appears that a proportion of POS may be trafficked outside the conventional pathway via other mechanisms. It will be interesting to determine whether this low level of flexibility and variation in POS trafficking/processing also exists under in-vivo conditions as it could have significant implications for understanding the susceptibility of RPE to proteolytic damage.

POS trafficking was significantly altered when RPE were subject to oxidative stress utilizing a well-established method used by others [29, 63]. The amount of H_2O_2 used was also similar to their concentration in the human vitreous [28]. We observed markedly diminished levels of POS in Rab5 and Rab7 vesicles compared to heathy RPE. We attributed this to the rapid trafficking of cargos to early and mature lysosomes as well as LC3b labelled compartments. POS cargos could bypass early and intermediate compartments under conditions of oxidative stress to prematurely co-localise with apical lysosomes. Such apically distributed lysosomes have been reported in proximity to RPE microvilli in a rat model of inherited retinopathy [64]. Although the Costes method [32] provides a direct readout of the incidence/extent of co-localisation, it cannot measure the amount of POS in each compartment. Consequently, we were unable to determine whether prematurely targeted POS remained sequestered in lysosomes and autophagosomes from early time points. However, rapid trafficking of POS that had bypassed upstream processing events may contribute to the likelihood of proteolytically indigestible material accumulating within RPE lysosomes, and a potential mechanism for lipofuscin biogenesis, as once formed, lipofuscin is considered to be resistant to degradation and cannot be transported outside the cell by exocytosis [65]. Indeed the accumulation of high molecular weight aggregates within lysosomes and related organelles is a major feature of degenerative conditions such as Alzheimer's disease and AMD [15, 18, 66, 67]. We measured the size of compartments in oxidatively stressed and heathy RPE, which revealed a significant increase in the size of LAMP1 and LAMP2 labelled vesicles as well as autophagosomes carrying POS from early time points. This is consistent with enlarged and swollen lysosomes reported in neurons of Alzheimer's patients, which is one of the earliest neuropathological features that appear decades before symptoms [68]. Of note, the size of lysosomes without POS cargos in oxidatively stressed RPE remained normal, suggesting a mechanism in which only those vesicles carrying POS are affected.

Impaired acidification of lysosomes is thought to result in inefficient fusion between lysosomes and autophagosomes which leads to dysregulated autophagy [22, 23]. There is ample evidence to support disrupted acidification of RPE lysosomes in retinopathies [69-71]. Lysosomal fusion can also be disrupted by other mechanisms although there is no evidence that all these necessarily occur in RPE cells. For instance, we have shown that loss of MYO1C/myosin 1c involved in the distribution of lipid rafts impairs lysosome-autophagosome fusion [72]. Whether by an increase in acidity or by alkalinisation of lysosomes, fusion with autophagosomes is nonetheless disrupted, since this is dependent on specific intra-lysosomal conditions [35]. This process is likely to be highly specific as the accumulation of A2-E, for instance, does not lead to lysosomal pH changes or inhibit activity of lysosomal enzymes in the RPE [21]. In a further complication, the accumulation of high molecular weight proteins including lipofuscin, A2-E, Aβ, HNE and MDA can also generate free radicals and disrupt lysosomes [20, 31, 49, 73-75]. We have previously shown how misfolded proteins rupture lysosomal membranes in diseased neurons [76]. Unsurprisingly, analysis of donor tissues from AMD patients show evidence of dysregulated autophagy including presence of the autophagy marker Atg5 and exosome markers CD36, CD81 and LAMP1 in drusen [16]. Upregulation of LC3, Atg7 and Atg9A are also reported in RPE of donor AMD patients, although LC3 appeared diminished during early stages of disease [29]. We treated cultured RPE with bafilomycin A^1 to disrupt lysosomal acidification in order to prevent fusion with autophagosomes and disrupt maturation along the endocytic pathway. We observed significantly high levels of POS in Rab5 and Rab7 vesicles at late time points (12-48 hours), which was in sharp contrast to cargos being trafficked away from these compartments in heathy RPE. POS therefore appeared to be sequestered in early and late phagosomes/endosomes, which was supported by our observation that cargos failed to be subsequently trafficked to LAMP1/2 lysosomes. Although we cannot directly comment on whether POS were sequestered in Rab5 and Rab7 compartments per se, we recorded a significant increase in the size of POS positive phagosomes/endosomes whilst the size of lysosomes were markedly smaller compared to heathy RPE. In contrast, the size of Rab5,

Rab7 and lysosomes devoid of POS in bafilomycin treated cells were broadly similar to their counterparts in untreated/heathy RPE, indicating a cargo-specific effect. Enlarged endosomes is a known feature of early stages of neuropathological conditions such as Alzheimer's disease and Down syndrome where misfolded proteins principally localise to Rab5 vesicles [68]. Swollen endosomes are also reported in RPE of aged human donors and Abca4$^{-/-}$ mouse model of Stargardt disease [77]. The failure of POS cargos to reach terminal stages of the proteolytic pathway could lead to their accumulation in RPE cells. The importance of lytic compartments to retinal function was demonstrated by findings showing high levels of lysosomal cathepsin D and acid phosphatase in macular RPE cells relative to RPE in the nasal/mid-zone and peripheral retina. Lysosomal enzyme activity also decreased by ~50% when exposed to lipofuscin, suggesting vulnerability of macular RPE to intracellular protein aggregation [75, 78]. Although a large proportion of POS failed to be trafficked to lysosomes, we noticed a significant increase in LC3b labelled compartments from early time points. Our results indicate that a proportion of POS cargos had bypassed the conventional trafficking pathway, suggesting a compensatory mechanism as a consequence of lysosomal dysfunction. Recent findings have revealed a non-canonical form of autophagy termed LC3-associated phagocytosis (LAP) [79, 80] through which lipidated LC3 associates with phagosomes in an Atg5 and Beclin1-dependent manner, but independently of the autophagy pre-initiation Alk1/Atg13/Fip200 complex. The importance of this pathway was demonstrated in mice lacking Atg5 where phagosomes contained undigested POS were unable to penetrate into the RPE. Phagocytosed POS also failed to associate with LAMP1/2 and cathepsin D, suggesting a role for Atg5 in POS trafficking to lysosomes. Furthermore, Atg5 deficient mice showed defective retinal function although there were no obvious damage to photoreceptors suggesting these effects are subtle but impact vision nonetheless [80]. Increased autophagy triggered by cyclical shedding of POS with at least part of the autophagy machinery directly involved in phagosome maturation may explain our observations in culture, although further studies are required to confirm this. The presence of significantly smaller sized LC3b compartments despite increased POS co-localisation in

bafilomycin treated RPE may indicate cargos associating with simpler membranes and evidence for non-canonical autophagy. Recent findings have shown that the LAP-specific mediator Rubicon (RUN domain and cysteine-rich domain consisting Beclin 1-interecting protein) can inhibit canonical autophagy, which raises the possibility of LAP vs. autophagy pathways competing for shared resources. Consequently, the daily internalisation of POS, particularly in aged RPE, adds another factor which requires regulation between LAP, canonical autophagy and phagocytosis to achieve homeostatic balance. Indeed, under starvation, RPE cells have been shown to activate autophagy in favour of phagocytosis [81]. The central role played by lysosomes under these conditions is therefore of growing interest. For instance, elimination of CRYBA1/βA3/A1-crstallin which regulates endo-lysosomal acidification, disrupted both autophagy and phagocytosis [82]. Recent work has also described links between proteasomal clearance and autophagy, as well as the importance of these processes to retinopathy. Hence, mice lacking NRF-2/ARE (nuclear factor-erythroid 2-related factor2/antioxidant response element) and PGC-1α (peroxisome proliferator-activated receptor γ co-activator 1) recapitulate salient features of GA [83]. Future studies will explore links between proteasomal clearance, autophagy and phagocytosis, and how these overlapping but divergent pathways function in our model. Impaired autophagy in the RPE also leads to inflammasome activation, angiogenesis and activation of innate immunity [15, 83, 84], linking dysfunction of cargo trafficking and clearance mechanisms with other well-recognised features of retinal degeneration.

In summary, this detailed study shows how POS cargos are tightly regulated and trafficked in the phagosome and autophagy-lysosomal pathways. Although a majority of cargos are transported in this manner, there appears to be some variability, perhaps indicating a degree of flexibility which could help RPE to cope with stressful conditions. The importance of correct cargo trafficking and timely proteolytic degradation is demonstrated by evidence from diverse neurodegenerative and storage diseases which reveal impairment of these

mechanisms in early stages of pathology [35, 68, 77, 85]. Our studies reveal divergent outcomes for POS trafficking under conditions of oxidative stress, impaired lysosomal function and disrupted autophagy (Fig. 7), all of which can occur simultaneously in the senescent RPE [86]. Some of these mechanisms may play a prominent role in retinas of certain patients whilst not in others, or indeed feature in different stages of disease. Furthermore, changes to the size of intracellular compartments largely correlated with the extent of POS co-localisation. Inconsistencies in this relationship, which occurred on occasion, were likely due to the dynamic nature of POS trafficking perhaps where cargos failed to spend sufficient periods in a given compartment to alter their size or morphology. Collectively, our findings illustrate some of the challenges in treating complex conditions such as AMD. Intriguingly, pathology appeared to be confined to vesicles containing POS, whilst the size of Rab5, Rab7, LAMP1/2 and LC3b compartments without cargos were broadly within normal parameters, suggesting a population of healthy compartments even in stressed or diseased RPE. These could be harnessed to rejuvenate RPE as an alternative approach for lysosomal rescue which has already been explored [87]. Our findings also provide new mechanistic insights into disease pathways underlying RPE-BrM pathology. Moreover, they provide further evidence for a central role for lysosomes, linking phagocytosis and autophagy, which has been considered separate processes in the past. Insights from this work also invite further questions to the manner in which endocytic compartments communicate with one another, and the origins and lifespan/turnover of lysosomes. Such questions are highly pertinent given recent findings demonstrating new functions of lysosomes in nutrient-sensing and metabolic homeostasis [61, 62], and the central role played by misfolded proteins and impaired clearance mechanisms in diseases such as Alzheimer's disease and AMD.

Author contributions

EK performed the experiments and analysed the data, DSC, DAJ and AP provided technical expertise. EK, DAT, AJL and JAR interpreted the findings. EK and JAR wrote the manuscript. DAT and AJL revised the manuscript.

Acknowledgements

This work was funded by awards to JAR from the Macular Society, the NC3R (NC/L001152/1), Retina UK (formally RP Fighting Blindness, GR590) and the Gift of Sight Appeal.

Conflict of interest

The authors declare no conflict of interest.

5 References

[1] Salas, I. H., Weerasekera, A., Ahmed, T., Callaerts-Vegh, Z*., et al.*, High fat diet treatment impairs hippocampal long-term potentiation without alterations of the core neuropathological features of Alzheimer disease. *Neurobiol Dis* 2018, *113*, 82-96.
[2] Chiu, C. J., Chang, M. L., Zhang, F. F., Li, T*., et al.*, The relationship of major American dietary patterns to age-related macular degeneration. *Am. J. Ophthalmol* 2014, *158*, 118-127.
[3] Datta, S., Cano, M., Ebrahimi, K., Wang, L., Handa, J. T., The impact of oxidative stress and inflammation on RPE degeneration in non-neovascular AMD. *Progress in retinal and eye research* 2017.
[4] Pikuleva, I. A., Curcio, C. A., Cholesterol in the retina: The best is yet to come. *Prog. Retin. Eye Res* 2014.
[5] Amoaku, W. M., Chakravarthy, U., Gale, R., Gavin, M*., et al.*, Defining response to anti-VEGF therapies in neovascular AMD. *Eye (Lond)* 2015, *29*, 721-731.
[6] Khandhadia, S., Cherry, J., Lotery, A. J., Age-related macular degeneration. *Adv. Exp. Med. Biol* 2012, *724*, 15-36.
[7] Wong, W. L., Su, X., Li, X., Cheung, C. M*., et al.*, Global prevalence of age-related macular degeneration and disease burden projection for 2020 and 2040: a systematic review and meta-analysis. *The Lancet. Global health* 2014, *2*, e106-116.
[8] Hogg, R. E., Woodside, J. V., McGrath, A., Young, I. S*., et al.*, Mediterranean Diet Score and Its Association with Age-Related Macular Degeneration: The European Eye Study. *Ophthalmology* 2017, *124*, 82-89.
[9] Merle, B. M., Silver, R. E., Rosner, B., Seddon, J. M., Adherence to a Mediterranean diet, genetic susceptibility, and progression to advanced macular degeneration: a prospective cohort study. *The American journal of clinical nutrition* 2015, *102*, 1196-1206.
[10] Seddon, J. M., Cote, J., Rosner, B., Progression of age-related macular degeneration: association with dietary fat, transunsaturated fat, nuts, and fish intake. *Archives of ophthalmology (Chicago, Ill. : 1960)* 2003, *121*, 1728-1737.

[11] Gorusupudi, A., Nelson, K., Bernstein, P. S., The Age-Related Eye Disease 2 Study: Micronutrients in the Treatment of Macular Degeneration. *Advances in nutrition (Bethesda, Md.)* 2017, *8*, 40-53.
[12] Rowan, S., Taylor, A., Gene-Diet Interactions in Age-Related Macular Degeneration. *Adv Exp Med Biol* 2016, *854*, 95-101.
[13] Curcio, C. A., Johnson, M., Huang, J. D., Rudolf, M., Apolipoprotein B-containing lipoproteins in retinal aging and age-related macular degeneration. *Journal of lipid research* 2010, *51*, 451-467.
[14] Curcio, C. A., Johnson, M., Rudolf, M., Huang, J. D., The oil spill in ageing Bruch membrane. *Br. J. Ophthalmol* 2011, *95*, 1638-1645.
[15] Ferrington, D. A., Sinha, D., Kaarniranta, K., Defects in retinal pigment epithelial cell proteolysis and the pathology associated with age-related macular degeneration. *Progress in retinal and eye research* 2016, *51*, 69-89.
[16] Wang, A. L., Lukas, T. J., Yuan, M., Du, N.*, et al.*, Autophagy and exosomes in the aged retinal pigment epithelium: possible relevance to drusen formation and age-related macular degeneration. *PLoS. One* 2009, *4*, e4160.
[17] Anderson, D. M. G., Ablonczy, Z., Koutalos, Y., Hanneken, A. M.*, et al.*, Bis(monoacylglycero)phosphate lipids in the retinal pigment epithelium implicate lysosomal/endosomal dysfunction in a model of Stargardt disease and human retinas. *Sci Rep* 2017, *7*, 17352.
[18] Feeney-Burns, L., Hilderbrand, E. S., Eldridge, S., Aging human RPE: morphometric analysis of macular, equatorial, and peripheral cells. *Invest Ophthalmol. Vis. Sci* 1984, *25*, 195-200.
[19] Beatty, S., Koh, H., Phil, M., Henson, D., Boulton, M., The role of oxidative stress in the pathogenesis of age-related macular degeneration. *Survey of ophthalmology* 2000, *45*, 115-134.
[20] Rozanowska, M., Jarvis-Evans, J., Korytowski, W., Boulton, M. E.*, et al.*, Blue light-induced reactivity of retinal age pigment. In vitro generation of oxygen-reactive species. *J Biol Chem* 1995, *270*, 18825-18830.
[21] Lakkaraju, A., Finnemann, S. C., Rodriguez-Boulan, E., The lipofuscin fluorophore A2E perturbs cholesterol metabolism in retinal pigment epithelial cells. *Proceedings of the National Academy of Sciences of the United States of America* 2007, *104*, 11026-11031.
[22] Las, G., Serada, S. B., Wikstrom, J. D., Twig, G., Shirihai, O. S., Fatty acids suppress autophagic turnover in beta-cells. *J Biol Chem* 2011, *286*, 42534-42544.
[23] Koga, H., Kaushik, S., Cuervo, A. M., Altered lipid content inhibits autophagic vesicular fusion. *Faseb j* 2010, *24*, 3052-3065.
[24] Dunn, K. C., Aotaki-Keen, A. E., Putkey, F. R., Hjelmeland, L. M., ARPE-19, a human retinal pigment epithelial cell line with differentiated properties. *Exp. Eye Res* 1996, *62*, 155-169.
[25] Ahmado, A., Carr, A. J., Vugler, A. A., Semo, M.*, et al.*, Induction of differentiation by pyruvate and DMEM in the human retinal pigment epithelium cell line ARPE-19. *Invest Ophthalmol Vis Sci* 2011, *52*, 7148-7159.
[26] Lynn, S. A., Keeling, E., Dewing, J. M., Johnston, D. A.*, et al.*, A convenient protocol for establishing a human cell culture model of the outer retina. *F1000Research* 2018, *7*, 1107.
[27] Bergmann, M., Holz, F., Kopitz, J., Lysosomal stress and lipid peroxidation products induce VEGF-121 and VEGF-165 expression in ARPE-19 cells. *Graefes Arch Clin Exp Ophthalmol* 2011, *249*, 1477-1483.
[28] Halliwell, B., Clement, M. V., Long, L. H., Hydrogen peroxide in the human body. *FEBS Lett* 2000, *486*, 10-13.
[29] Mitter, S. K., Song, C., Qi, X., Mao, H.*, et al.*, Dysregulated autophagy in the RPE is associated with increased susceptibility to oxidative stress and AMD. *Autophagy* 2014, *10*, 1989-2005.
[30] Hall, M. O., Abrams, T., Kinetic studies of rod outer segment binding and ingestion by cultured rat RPE cells. *Exp Eye Res* 1987, *45*, 907-922.
[31] Krohne, T. U., Stratmann, N. K., Kopitz, J., Holz, F. G., Effects of lipid peroxidation products on lipofuscinogenesis and autophagy in human retinal pigment epithelial cells. *Exp. Eye Res* 2010, *90*, 465-471.

[32] Costes, S. V., Daelemans, D., Cho, E. H., Dobbin, Z.*, et al.*, Automatic and quantitative measurement of protein-protein colocalization in live cells. *Biophysical journal* 2004, *86*, 3993-4003.
[33] Bright, N. A., Davis, L. J., Luzio, J. P., Endolysosomes Are the Principal Intracellular Sites of Acid Hydrolase Activity. *Current biology : CB* 2016, *26*, 2233-2245.
[34] Lynn, S. A., Ward, G., Keeling, E., Scott, J. A.*, et al.*, Ex-vivo models of the Retinal Pigment Epithelium (RPE) in long-term culture faithfully recapitulate key structural and physiological features of native RPE. *Tissue & cell* 2017, *49*, 447-460.
[35] Keeling, E., Lotery, A. J., Tumbarello, D. A., Ratnayaka, J. A., Impaired Cargo Clearance in the Retinal Pigment Epithelium (RPE) Underlies Irreversible Blinding Diseases. *Cells* 2018, *7*.
[36] Bucci, C., Thomsen, P., Nicoziani, P., McCarthy, J., van Deurs, B., Rab7: a key to lysosome biogenesis. *Molecular biology of the cell* 2000, *11*, 467-480.
[37] Humphries, W. H. t., Szymanski, C. J., Payne, C. K., Endo-lysosomal vesicles positive for Rab7 and LAMP1 are terminal vesicles for the transport of dextran. *PloS one* 2011, *6*, e26626.
[38] Barathi, V. A., Yeo, S. W., Guymer, R. H., Wong, T. Y., Luu, C. D., Effects of simvastatin on retinal structure and function of a high-fat atherogenic mouse model of thickened Bruch's membrane. *Invest Ophthalmol. Vis. Sci* 2014, *55*, 460-468.
[39] Dasari, B., Prasanthi, J. R., Marwarha, G., Singh, B. B., Ghribi, O., Cholesterol-enriched diet causes age-related macular degeneration-like pathology in rabbit retina. *BMC. Ophthalmol* 2011, *11*, 22.
[40] Chang, R. C., Shi, L., Huang, C. C., Kim, A. J.*, et al.*, High-Fat Diet-Induced Retinal Dysfunction. *Invest Ophthalmol. Vis. Sci* 2015, *56*, 2367-2380.
[41] Miceli, M. V., Newsome, D. A., Tate, D. J., Jr., Sarphie, T. G., Pathologic changes in the retinal pigment epithelium and Bruch's membrane of fat-fed atherogenic mice. *Curr Eye Res* 2000, *20*, 8-16.
[42] Malek, G., Johnson, L. V., Mace, B. E., Saloupis, P.*, et al.*, Apolipoprotein E allele-dependent pathogenesis: a model for age-related retinal degeneration. *Proc. Natl. Acad. Sci. U. S. A* 2005, *102*, 11900-11905.
[43] Tan, L. X., Toops, K. A., Lakkaraju, A., Protective responses to sublytic complement in the retinal pigment epithelium. *Proceedings of the National Academy of Sciences of the United States of America* 2016, *113*, 8789-8794.
[44] Johnson, L. V., Forest, D. L., Banna, C. D., Radeke, C. M.*, et al.*, Cell culture model that mimics drusen formation and triggers complement activation associated with age-related macular degeneration. *Proc. Natl. Acad. Sci. U. S. A* 2011, *108*, 18277-18282.
[45] Shaw, P. X., Zhang, L., Zhang, M., Du, H.*, et al.*, Complement factor H genotypes impact risk of age-related macular degeneration by interaction with oxidized phospholipids. *Proceedings of the National Academy of Sciences of the United States of America* 2012, *109*, 13757-13762.
[46] Suzuki, M., Kamei, M., Itabe, H., Yoneda, K.*, et al.*, Oxidized phospholipids in the macula increase with age and in eyes with age-related macular degeneration. *Mol Vis* 2007, *13*, 772-778.
[47] Hoppe, G., O'Neil, J., Hoff, H. F., Sears, J., Accumulation of oxidized lipid-protein complexes alters phagosome maturation in retinal pigment epithelium. *Cell Mol Life Sci* 2004, *61*, 1664-1674.
[48] Schutt, F., Bergmann, M., Holz, F. G., Kopitz, J., Proteins modified by malondialdehyde, 4-hydroxynonenal, or advanced glycation end products in lipofuscin of human retinal pigment epithelium. *Invest Ophthalmol. Vis. Sci* 2003, *44*, 3663-3668.
[49] Kaemmerer, E., Schutt, F., Krohne, T. U., Holz, F. G., Kopitz, J., Effects of lipid peroxidation-related protein modifications on RPE lysosomal functions and POS phagocytosis. *Invest Ophthalmol. Vis. Sci* 2007, *48*, 1342-1347.
[50] Krohne, T. U., Holz, F. G., Kopitz, J., Apical-to-basolateral transcytosis of photoreceptor outer segments induced by lipid peroxidation products in human retinal pigment epithelial cells. *Invest Ophthalmol. Vis. Sci* 2010, *51*, 553-560.
[51] Krohne, T. U., Kaemmerer, E., Holz, F. G., Kopitz, J., Lipid peroxidation products reduce lysosomal protease activities in human retinal pigment epithelial cells via two different mechanisms of action. *Exp. Eye Res* 2010, *90*, 261-266.

[52] Rakoczy, P. E., Sarks, S. H., Daw, N., Constable, I. J., Distribution of cathepsin D in human eyes with or without age-related maculopathy. *Exp. Eye Res* 1999, *69*, 367-374.
[53] Bhattacharya, S., Yin, J., Winborn, C. S., Zhang, Q.*, et al.*, Prominin-1 Is a Novel Regulator of Autophagy in the Human Retinal Pigment Epithelium. *Invest Ophthalmol Vis Sci* 2017, *58*, 2366-2387.
[54] Wavre-Shapton, S. T., Tolmachova, T., Lopes da Silva, M., Futter, C. E., Seabra, M. C., Conditional ablation of the choroideremia gene causes age-related changes in mouse retinal pigment epithelium. *PloS one* 2013, *8*, e57769.
[55] Young, R. W., Bok, D., Participation of the retinal pigment epithelium in the rod outer segment renewal process. *J Cell Biol* 1969, *42*, 392-403.
[56] Young, R. W., The renewal of rod and cone outer segments in the rhesus monkey. *J Cell Biol* 1971, *49*, 303-318.
[57] Finnemann, S. C., Leung, L. W., Rodriguez-Boulan, E., The lipofuscin component A2E selectively inhibits phagolysosomal degradation of photoreceptor phospholipid by the retinal pigment epithelium. *Proc. Natl. Acad. Sci. U. S. A* 2002, *99*, 3842-3847.
[58] Finnemann, S. C., Nandrot, E. F., MerTK activation during RPE phagocytosis in vivo requires alphaVbeta5 integrin. *Adv Exp Med Biol* 2006, *572*, 499-503.
[59] Klionsky, D. J., Abdelmohsen, K., Abe, A., Abedin, M. J.*, et al.*, Guidelines for the use and interpretation of assays for monitoring autophagy (3rd edition). *Autophagy* 2016, *12*, 1-222.
[60] Mazzoni, F., Safa, H., Finnemann, S. C., Understanding photoreceptor outer segment phagocytosis: use and utility of RPE cells in culture. *Exp Eye Res* 2014, *126*, 51-60.
[61] Lim, C. Y., Zoncu, R., The lysosome as a command-and-control center for cellular metabolism. *J Cell Biol* 2016, *214*, 653-664.
[62] Luzio, J. P., Hackmann, Y., Dieckmann, N. M., Griffiths, G. M., The biogenesis of lysosomes and lysosome-related organelles. *Cold Spring Harbor perspectives in biology* 2014, *6*, a016840.
[63] Ryhanen, T., Hyttinen, J. M., Kopitz, J., Rilla, K.*, et al.*, Crosstalk between Hsp70 molecular chaperone, lysosomes and proteasomes in autophagy-mediated proteolysis in human retinal pigment epithelial cells. *J. Cell Mol. Med* 2009, *13*, 3616-3631.
[64] Essner, E., Gorrin, G. M., Griewski, R. A., Localization of lysosomal enzymes in retinal pigment epithelium of rats with inherited retinal dystrophy. *Invest Ophthalmol Vis Sci* 1978, *17*, 278-288.
[65] Jung, T., Bader, N., Grune, T., Lipofuscin: formation, distribution, and metabolic consequences. *Annals of the New York Academy of Sciences* 2007, *1119*, 97-111.
[66] Kaarniranta, K., Hyttinen, J., Ryhanen, T., Viiri, J.*, et al.*, Mechanisms of protein aggregation in the retinal pigment epithelial cells. *Front Biosci. (Elite. Ed)* 2010, *2*, 1374-1384.
[67] Hyttinen, J. M., Amadio, M., Viiri, J., Pascale, A.*, et al.*, Clearance of misfolded and aggregated proteins by aggrephagy and implications for aggregation diseases. *Ageing research reviews* 2014, *18*, 16-28.
[68] Cataldo, A. M., Petanceska, S., Terio, N. B., Peterhoff, C. M.*, et al.*, Abeta localization in abnormal endosomes: association with earliest Abeta elevations in AD and Down syndrome. *Neurobiol. Aging* 2004, *25*, 1263-1272.
[69] Guha, S., Coffey, E. E., Lu, W., Lim, J. C.*, et al.*, Approaches for detecting lysosomal alkalinization and impaired degradation in fresh and cultured RPE cells: evidence for a role in retinal degenerations. *Exp. Eye Res* 2014, *126*, 68-76.
[70] Bergmann, M., Schutt, F., Holz, F. G., Kopitz, J., Inhibition of the ATP-driven proton pump in RPE lysosomes by the major lipofuscin fluorophore A2-E may contribute to the pathogenesis of age-related macular degeneration. *FASEB J* 2004, *18*, 562-564.
[71] Guha, S., Baltazar, G. C., Coffey, E. E., Tu, L. A.*, et al.*, Lysosomal alkalinization, lipid oxidation, and reduced phagosome clearance triggered by activation of the P2X7 receptor. *Faseb j* 2013, *27*, 4500-4509.
[72] Brandstaetter, H., Kishi-Itakura, C., Tumbarello, D. A., Manstein, D. J., Buss, F., Loss of functional MYO1C/myosin 1c, a motor protein involved in lipid raft trafficking, disrupts autophagosome-lysosome fusion. *Autophagy* 2014, *10*, 2310-2323.

[73] Liu, R. Q., Zhou, Q. H., Ji, S. R., Zhou, Q.*, et al.*, Membrane localization of beta-amyloid 1-42 in lysosomes: a possible mechanism for lysosome labilization. *J. Biol. Chem* 2010, *285*, 19986-19996.
[74] Davies, S., Elliott, M. H., Floor, E., Truscott, T. G.*, et al.*, Photocytotoxicity of lipofuscin in human retinal pigment epithelial cells. *Free Radic. Biol. Med* 2001, *31*, 256-265.
[75] Shamsi, F. A., Boulton, M., Inhibition of RPE lysosomal and antioxidant activity by the age pigment lipofuscin. *Invest Ophthalmol. Vis. Sci* 2001, *42*, 3041-3046.
[76] Soura, V., Stewart-Parker, M., Williams, T. L., Ratnayaka, A.*, et al.*, Visualization of co-localization in Abeta42-administered neuroblastoma cells reveals lysosome damage and autophagosome accumulation related to cell death. *Biochem. J* 2012, *441*, 579-590.
[77] Kaur, G., Tan, L. X., Rathnasamy, G., La Cunza, N.*, et al.*, Aberrant early endosome biogenesis mediates complement activation in the retinal pigment epithelium in models of macular degeneration. *Proceedings of the National Academy of Sciences of the United States of America* 2018, *115*, 9014-9019.
[78] Boulton, M., Moriarty, P., Jarvis-Evans, J., Marcyniuk, B., Regional variation and age-related changes of lysosomal enzymes in the human retinal pigment epithelium. *Br. J. Ophthalmol* 1994, *78*, 125-129.
[79] Heckmann, B. L., Boada-Romero, E., Cunha, L. D., Magne, J., Green, D. R., LC3-Associated Phagocytosis and Inflammation. *Journal of molecular biology* 2017, *429*, 3561-3576.
[80] Kim, J. Y., Zhao, H., Martinez, J., Doggett, T. A.*, et al.*, Noncanonical autophagy promotes the visual cycle. *Cell* 2013, *154*, 365-376.
[81] Muniz-Feliciano, L., Doggett, T. A., Zhou, Z., Ferguson, T. A., RUBCN/rubicon and EGFR regulate lysosomal degradative processes in the retinal pigment epithelium (RPE) of the eye. *Autophagy* 2017, *13*, 2072-2085.
[82] Valapala, M., Wilson, C., Hose, S., Bhutto, I. A.*, et al.*, Lysosomal-mediated waste clearance in retinal pigment epithelial cells is regulated by CRYBA1/betaA3/A1-crystallin via V-ATPase-MTORC1 signaling. *Autophagy* 2014, *10*, 480-496.
[83] Felszeghy, S., Viiri, J., Paterno, J. J., Hyttinen, J. M. T.*, et al.*, Loss of NRF-2 and PGC-1alpha genes leads to retinal pigment epithelium damage resembling dry age-related macular degeneration. *Redox biology* 2019, *20*, 1-12.
[84] Liu, J., Copland, D. A., Theodoropoulou, S., Chiu, H. A.*, et al.*, Impairing autophagy in retinal pigment epithelium leads to inflammasome activation and enhanced macrophage-mediated angiogenesis. *Sci Rep* 2016, *6*, 20639.
[85] Hu, X., Crick, S. L., Bu, G., Frieden, C.*, et al.*, Amyloid seeds formed by cellular uptake, concentration, and aggregation of the amyloid-beta peptide. *Proc. Natl. Acad. Sci. U. S. A* 2009, *106*, 20324-20329.
[86] Kaarniranta, K., Tokarz, P., Koskela, A., Paterno, J., Blasiak, J., Autophagy regulates death of retinal pigment epithelium cells in age-related macular degeneration. *Cell biology and toxicology* 2017, *33*, 113-128.
[87] Guha, S., Liu, J., Baltazar, G., Laties, A. M., Mitchell, C. H., Rescue of compromised lysosomes enhances degradation of photoreceptor outer segments and reduces lipofuscin-like autofluorescence in retinal pigmented epithelial cells. *Adv Exp Med Biol* 2014, *801*, 105-111.

Figure legends

Figure 1. The Retinal Pigment Epithelium (RPE) and trafficking of photoreceptor outer segment cargos in the endo-lysosomal and autophagy pathway. [A] Schematic of the retina and associated layers illustrating juxtaposition of the RPE monolayer (inset box) between the

neuroretina and the supportive Bruch's membrane (BrM) and choroid. Formation of subretinal protein/lipid deposits referred to as drusen under the RPE in the central retina (the macula) is associated with a high risk of developing retinopathy. [B] Schematic diagram illustrating the pathway through which photoreceptor outer segment (POS) cargos bind to receptors on RPE cells and are processed via the phagosome, endosome and lysosomal-autophagy pathway. Early compartments are labelled with Rab5 and late compartments with Rab7. Lysosomes are indicated by LAMP 1 and 2 markers, whilst autophagy bodies are labelled with LC3b. Isolated POS are fluorescently labelled and can be used to study effects of disease conditions on cargo trafficking in cultured RPE. [C] Representative confocal image taken after POS feeding and rendered in 3D showing bound POS molecules (green) on the RPE cell surface which co-localise with receptor MerTK (red) and $\alpha v\beta 5$ integrin (grey) indicated by arrows. A wash step ensures the removal of any unbound cargos so that only receptor-bound POS are subsequently internalised. Some $\alpha v\beta 5$ receptors that have not bound to POS are visible in grey. Scale bar corresponds to 20μm. [D] Representative confocal image taken at 4 hours after feeding assay showing early trafficking of POS cargos (green) in Rab5 (red) compartments. Co-localised vesicles appear yellow. Scale bar corresponds to 30μm. [E] Representative confocal image taken 6 hours after feeding assay showing trafficking of POS cargo (green) in Rab7 (red) vesicles. Co-localised compartments appear yellow. Scale bar corresponds to 30μm. [F] Representative confocal images collected at 24 hours after the feeding assay showed POS cargo (green) predominantly co-localised to LAMP1 (red) and [G] LAMP2 (red) labelled compartments. Lysosomes containing POS molecules appear yellow. Note the perinuclear arrangement of lysosomes trafficking POS cargos. Scale bars in panels F and G correspond to 15μm and 20μm respectively. [H] Representative confocal image taken at 48 hours after feeding assay showed that by this stage most POS cargos (green) had been trafficked to LC3b positive (red) compartments. Co-localisation is indicated in yellow. Scale bar corresponds to 25μm. Nuclei in panels C-H are labelled with DAPI and appear blue. The image in panel C was

rendered in 3D using Leica software on a SP8 confocal microscope. Panels D-H show three-dimensional RPE monolayers with intracellular cargo which were captured using a confocal microscope and reconstructed using Amira software.

Figure 2. The trafficking of POS cargos in heathy RPE cells. The trafficking of internalised POS molecules in phagosomes/endosomes and in the lysosomal-autophagy pathway was studied using an automated, unbiased quantification method described by Costes *et al*. The extent of co-localisation in distinct compartments at each time point is shown as mean values (1.0 represents 100% co-localisation). [A] The trafficking of POS cargos in Rab5 labelled vesicles peaked between 2-6 hours following the feeding assay with the maximum extent of co-localisation at 4 hours after which values returned to significantly lower levels by 12 hours. [B] Although some cargos had entered Rab7 labelled vesicles as early as 2-4 hours, the highest extent of co-localisation was recorded at 6 hours after which they declined in successive time points. [C] From early on, a small proportion of POS cargos appeared to be trafficked to LAMP1 positive lysosomes, which increased gradually with each time point. However, peak levels of trafficking was observed between 12-48 hours with the maximal extent of co-localisation recorded at 24 hours. [D] In contrast, the small proportion of POS cargos trafficked to LAMP2 positive vesicles at early time points (2-6 hours) remained constant. However, the extent of co-localisation increased significantly thereafter at 12 hours and followed a similar pattern observed in early (LAMP1) lysosomes. [E] A small number of POS cargos appeared to co-localise with LC3b labelled membranes between 2-6 hours after the feeding assay. The extent of trafficking to LC3b positive compartments increased significantly thereafter at 12 hours and continued to increase at each time point to record the maximal extent of co-localisation at 48 hours. Error bars represent the standard deviation. Data from four independent experiments with a minimum of n=20 cells/time point. Statistical comparisons using ANOVA where a significance of $p < 0.05$ (*), $p < 0.01$ (**) and at least $p < 0.001$ (***) was recorded with the previous time point in the assay.

Figure 3. Vesicle dynamics in the trafficking pathway and evidence of POS trafficking at ultrastructural resolution in RPE cells. [A] Lysosomes of living RPE were labelled with CellLite Lysosomes-RFP (red) after which cultures were probed with an antibody against Rab7 (green). This revealed distinct populations of lysosomes and Rab7 labelled late compartments. However, we detected lysosomes that were also positive for Rab7 (co-localisation indicated by yellow). Representative image from a single plane of a confocal z-stack where crossbar indicate co-localisation (orthogonal view shows co-labelling marked by a white arrow). Scale bar corresponds to 25μm. [B] Evidence for cargo trafficking was assessed by transmission electron microscopy in heathy RPE after POS feeding. Representative electron micrograph at the 2 hour time point following feeding showing numerous POS containing early compartments (white arrows). There is evidence that some cargos had been trafficked to late compartments (yellow arrowhead) at this early stage. Scale bar corresponds to 500nm. [C] Electron micrograph taken 6 hours after the feeding assay shows that most cargos had already been trafficked to late compartments (yellow arrowheads), although there was still some evidence of POS in early vesicles (white arrow). Scale bar corresponds to 500nm. [D] Representative micrograph from 12 hours following the feeding assay showing POS cargos in late compartments (yellow arrowhead). There were no obvious indication of any cargos in early compartments by this stage. Scale bar corresponds to 500nm. [E-F] 24 hours after the feeding assay cargos were observed localised to late compartments/lysosomes containing a mixture of partially degraded POS and electron dense material (yellow arrowheads). We found no evidence of any early compartments with POS at this late time point. [F] The presence of double membrane phagophores (black arrow) at the 24 hour time point indicate likely trafficking to autophagosomes. Scale bars in panels E and F correspond to 500nm.

Figure 4. High levels of oxidative stress in RPE cells causes premature trafficking of POS cargos to late compartments. The extent of co-localisation between internalised POS cargos and components of the proteolytic pathway was evaluated using an automated, unbiased

quantification method described by Costes *et al*. Data shown as mean values (1.0 represents 100% co-localisation). [A] The co-localisation of POS cargos to Rab5 labelled vesicles in cells treated with 100μM H_2O_2 show a significant reduction during early time points (2-6 hours) compared to controls. This low level of Rab5 co-localisation remained constant throughout the experiment, although this meant that a proportion of cargos remained in these early compartments even at late time points. [B] Trafficking of cargos to Rab7 vesicles show a similar pattern where only a small proportion localised within these late compartments throughout the time course compared to controls. [C] Treatment with100μM H_2O_2 however significantly increase the proportion of POS cargos that were co-localised to LAMP1 and [D] LAMP2 lysosomes compared to controls. [E] A substantial proportion of POS cargos also co-localised with LC3b labelled vesicles at early time points, which continued to increase further at each time point compared to untreated control cultures. Error bars represent the standard deviation. Data from three independent experiments with a minimum of n=15 cells/time point. Statistical comparisons using a two-tailed unpaired Student's t-test comparing differences between conditions for each time point. * denotes a significance of $p < 0.05$ whilst *** indicated a significance of at least $p < 0.001$.

Figure 5. Dysregulated autophagy in the RPE leads to POS cargos being sequestered in early vesicles whilst a proportion of cargos are prematurely trafficked to LC3b positive compartments. The extent of co-localisation between POS and intracellular compartments was evaluated using an automated, unbiased quantification method described by Costes *et al* and shown as mean values (1.0 represents 100% co-localisation). [A] Exposure of cultured RPE cells to 10nM bafilomycin results in a large proportion of POS cargos being retained in Rab5 and [B] Rab7 labelled vesicles compared to untreated controls. [C] POS cargos remain sequestered in early compartments and fail to be trafficked to lysosomes. Consequently, only a small proportion of cargos co-localise with LAMP1 and [D] LAMP2

lysosomes compared to controls. This effect appeared exaggerated in LAMP2 compartments, which remain at a constantly low level throughout all time points. [E] A significant proportion of POS cargos appear to co-localise with LC3b labelled compartments at early time points (4-12 hours) compared to untreated cells. The level of co-localisation with this autophagy marker increased thereafter at each time point until they had reached a similar level to heathy RPE by 48 hours after the feeding assay. Error bars represent the standard deviation. Data from three independent experiments with a minimum of n=15 cells/time point. Statistical comparisons using a two-tailed unpaired Student's t-test comparing differences between conditions for each time point. * denotes a significance of $p < 0.05$, ** indicates $p < 0.01$ whilst *** shows a significance of at least $p < 0.001$.

Figure 6. Effects of high oxidative stress and dysregulated autophagy on the size of intracellular compartments in the POS trafficking pathway. Potential effects of H_2O_2 or bafilomycin treatment were assessed by quantifying the size of POS-trafficking intracellular compartments in RPE cells. [A] Effects of H_2O_2 on the Rab5 early compartment show enlarged vesicles at 6 and 24 hours compared to untreated cells. [B] Exposure to H_2O_2 had no appreciable effects on the size of Rab7 vesicles until 48 hours. [C] By contrast, treatment with H_2O_2 led to a significant increase in the size of early and [D] late lysosomes. Enlarged early lysosomes were observed from the first time point of 2 hours after POS feeding. However, differences with normal lysosomes were most obvious at later time points. [E] An increase in the sizes of autophagy bodies over those present in heathy cells were also detected as a consequence of H_2O_2 treatment. [F] Effects of bafilomycin treatment on Rab5 labelled vesicles show a significant increase in the size of compartments over those in control cells from 6 hours onwards. [G] A similar effect was observed in Rab7 vesicles but from the first time point of 2 hours. [H] In contrast, treatment with bafilomycin significantly reduced the size of early and [I] late lysosomes. This effect was obvious in late lysosomes from the first time point of 2 hours. However, swollen lysosomes returned to normal levels by 48 hours. [J] Exposure to bafilomycin also resulted in a significant decrease in the size of

LC3b labelled autophagy compartments over those in untreated cells. Error bars represent the standard deviation. Images collected from three independent experiments. n=15 separate measurements for each marker per time point. * denotes a significance of $p < 0.05$, ** indicates $p < 0.01$ whilst *** shows a significance of at least $p < 0.001$.

Figure 7. Summary diagram illustrating the fate of photoreceptor outer segment (POS) trafficking under conditions of high oxidative stress and dysregulated autophagy in the RPE. Extent of POS co-localisation in distinct intracellular compartments are mathematically represented, which show sequential shuttling of cargos from early (Rab5) and late phagosomes/endosomes (Rab7) to immature (LAMP1) and mature lysosomes (LAMP2) before delivery to autophagosomes (LC3b). High oxidative stress leads to the rapid and premature trafficking of POS to late compartments. In contrast, dysregulated autophagy results in POS being sequestered in early compartments for long periods. Only a small proportion of cargos appear to reach lysosomes. Some POS however, appear to prematurely co-localise with LC3b labelled compartments. The diagram illustrate contrasting outcomes of two important pathogenic mechanisms triggered by an unhealthy diet and how they might contribute to disease in the RPE.